IEEE Access
Multidisciplinary : Rapid Review : Open Access Journal

Received February 2, 2020, accepted February 22, 2020, date of publication February 27, 2020, date of current version March 10, 2020.

Digital Object Identifier 10.1109/ACCESS.2020.2976732

Transmit Antenna Selection for Precoding-Aided Spatial Modulation

SANGCHOON KIM
Department of Electronics, Dong-A University, Busan 49315, South Korea
e-mail: sckim@dau.ac.kr

This work was supported by the Research Funds from Dong-A University.

ABSTRACT This paper examines the impacts of transmit antenna subset (TAS) selection on the bit-error-rate (BER) performance of linear precoding-aided spatial modulation (PSM) multiple-input multiple-output (MIMO) systems. It is analytically shown that decreasing the number of active transmit antennas by TAS selection, which can be used to reduce the number of RF units at the transmitter side, always degrades the BER performance. The expression of a received signal-to-noise ratio (SNR) loss is also derived and its analytical results are shown to be well-matched with simulation results. Furthermore, it is analyzed that when there are N_T transmit antennas, N_S selected transmit antennas, and N_R receive antennas, an achievable diversity order of the zero-forcing (ZF)-based PSM MIMO systems either with optimal TAS selection or without TAS selection can be given as $N_T - N_R + 1$. To select an optimal TAS based on exhaustive search, an optimization criterion to maximize the received SNR of the selected TAS is employed. In addition, a low-complexity TAS selection scheme is presented using a decremental strategy. It is also observed that the decremental TAS selection algorithm can achieve almost the same BER and achievable rate performance as the optimal one while attaining much lower complexity. Finally, simulation results show that under the identical number of active transmit antennas, the ZF-PSM MIMO system with TAS selection outperforms the conventional ZF-PSM without TAS selection.

INDEX TERMS Transmit antenna selection, multiple input multiple output (MIMO), precoding, zero-forcing (ZF), spatial modulation (SM).

I. INTRODUCTION

Spatial modulation (SM) is an attractive transmission scheme which allows multiple-input multiple-output (MIMO) communication systems to be implemented with low-complexity and low-cost [1]–[3]. In conventional SM, only one transmit antenna from N_T transmit antennas is activated for transmitting a symbol during a single symbol time. Extra information bits are conveyed by the index of the activated transmit antenna. Thus it has been known as transmit SM, where transmit antennas are considered to have a spatial constellation dimension. Recently, precoding-aided spatial modulation (PSM) [4]–[9] has been emerged as an extension of transmit SM. In a PSM scheme, the spatial position of each receive antenna is exploited as a source of information. It is also referred to as receive SM. Since a single receive antenna is activated at each time slot, the PSM scheme allows a simplified receiver design. To ensure the PSM design, the number of transmit antennas N_T should be equal to or larger than that of receive antennas N_R.

Antenna selection can be performed to use a limited number of expensive radio frequency (RF) chains while preserving spatial diversity gains [10]–[12]. Transmit antenna subset (TAS) selection techniques have recently been developed to introduce transmit diversity for the transmit SM systems and thus improve their reliability [13]–[15]. In [13] and [14], Euclidean distance (ED)-based TAS selection algorithms with low-complexity were presented. In [15], the transmit diversity order of transmit SM systems with ED-based TAS selection has been analyzed. More recently, receive antenna subset (RAS) selection [16], [17] has been investigated to enable the PSM in the over-determined MIMO systems ($N_T < N_R$). In [16], exhaustive search-based optimal algorithm and greedy incremental version are proposed to select

The associate editor coordinating the review of this manuscript and approving it for publication was Faisal Tariq.

an RAS for the PSM MIMO system. In [17], two efficient RAS selection approaches have been presented for the PSM system.

However, to the best of the author' knowledge, there are rarely prior researches on the impacts of TAS selection on the under-determined PSM-MIMO systems ($N_T > N_R$), where transmit diversity is always available. It seems that TAS selection for the PSM-MIMO systems has not yet been discussed. In [18] and [19], the use of all transmit antennas in precoded single-user MIMO systems does not always lead to the maximum throughput due to ill-conditioned channel matrices. Higher throughput can be obtained by removing these transmit antennas. On the other hand, it is shown in [20] that decreasing the number of active transmit antennas by TAS selection in linearly precoded multiuser MIMO systems always degrades the performance. This background is a motivation to examine whether similar results can be obtained in the under-determined PSM-MIMO systems. For a given number of transmit antennas N_T in practical under-determined PSM-MIMO systems, TAS selection can be performed to reduce the number of RF transmission units at the transmitter side.

In this paper, we analyze the bit error rate (BER) performance of TAS selection for zero-forcing (ZF)-based PSM MIMO systems with a limited number of RF transmission units at the transmitter side. It is analytically shown that decreasing the number of active transmit antennas always degrades the BER performance. Thus a received signal to noise ratio (SNR) loss is analytically derived and also shown to be matched with simulation results. For optimal TAS selection in the ZF-PSM MIMO systems, a criterion of minimizing their BER performance is used. It is equivalent to maximizing the received SNR of the selected TAS. It is pointed out in [20] that maximizing the sum throughput has been used for optimization of TAS selection. The optimal TAS selection based on exhaustive search requires prohibitive computational complexity when the number of transmit antennas is large. To significantly reduce the complexity of the optimal TAS selection algorithm, a decremental antenna selection strategy [21], [22] is employed. It is seen that the complexity-reduced decremental TAS selection algorithm can achieve the BER and achievable rate performance corresponding to the optimal scheme with much lower complexity. In addition, it is analytically shown that although decreasing the number of active transmit antennas for optimal TAS selection, an achievable transmit diversity order is the same as that of the ZF-PSM system without TAS selection, which is given by $N_T - N_R + 1$.

The remainder of this paper is organized as follows. In Section II, the conventional PSM system model with TAS selection is presented. In Section III, an achievable diversity order of the ZF-PSM MIMO system with TAS selection is analytically obtained. In Section IV, two TAS selection methods for the ZF-PSM MIMO system are introduced. The optimal TAS selection algorithm and complexity-reduced decremental TAS selection scheme are derived together with computational complexity analysis. Simulation results are presented in Section V. Finally, some conclusions are drawn in Section VI.

Notation: Throughout this paper, boldface lower and upper case letters represent vectors and matrices, respectively. $(\cdot)^T$, $(\cdot)^*$, and $(\cdot)^H$ denote the transpose, the complex conjugate, and the Hermitian transpose, respectively. $Tr(\cdot)$ and $(\cdot)^{-1}$ stand for the trace operation and inverse operation, respectively. $E[\cdot]$ and $\|\cdot\|$ denote the expectation and the Euclidean norm, respectively. $\mathbf{I}$, $|S|$, and $Q(\cdot)$ is the identity matrix, the size of a set S, and the Q function, respectively.

II. PSM SYSTEM WITH TAS SELECTION

Consider an under-determined MIMO system with N_T transmit antennas and N_R ($\leq N_T$) receive antennas. The transmitter is equipped with N_S ($N_R \leq N_S \leq N_T$) RF transmission units. The full channel matrix is given as $\mathbf{H} \in C^{N_R \times N_T}$, which is the quasi-static channel matrix whose elements are independent and identically distributed (i.i.d.) circularly symmetric complex Gaussian random variables with zero mean and unit variance. In this work, N_S antennas out of N_T transmit antennas are assumed to be selected. A spatial modulated super-symbol vector is presented by $\mathbf{x} \in C^{N_R \times 1}$, which can be expressed as $\mathbf{x} = s\,\mathbf{e}_r$ where a symbol s with $E[ss^*] = 1$ is selected from the M-ary quadrature amplitude modulation (QAM) or phase-shift keying (PSK) constellation set and $\mathbf{e}_r$ is the r-th column of the N_R-dimensional unit matrix. The super-symbol $\mathbf{x}$ is first precoded before transmission. Then the transmit signal vector is given by $\beta\,\mathbf{Px}$ where $\mathbf{P} \in C^{N_S \times N_R}$ is a pre-coding matrix and β is a power normalization factor used to ensure $E\left[\|\beta\,\mathbf{Px}\|^2\right] = 1$. In [5], [6], and [7], the ZF pre-coding scheme has been applied to PSM systems and the pre-coding matrix is

$$\mathbf{P}_{ZF} = \mathbf{H}_S^H\left(\mathbf{H}_S\mathbf{H}_S^H\right)^{-1} \tag{1}$$

where $\mathbf{H}_S \in C^{N_R \times N_S}$ denotes the channel matrix obtained by a transmit antenna subset (TAS) selection algorithm.

The received block signal at the receiver is described as

$$\begin{aligned} \mathbf{y} &= \beta_S\mathbf{H}_S\mathbf{Px} + \mathbf{n} \\ &= \beta_S\mathbf{x} + \mathbf{n} \end{aligned} \tag{2}$$

where the power normalization factor related with the selected TAS is

$$\beta_S = \sqrt{\frac{N_R}{Tr\left[\left(\mathbf{H}_S\mathbf{H}_S^H\right)^{-1}\right]}} \tag{3}$$

and $\mathbf{n} \in C^{N_R \times 1}$ is an i.i.d. additive white Gaussian noise vector whose elements are the zero-mean circular complex white Gaussian noise component of a variance of σ_n^2. Then the optimal maximum likelihood (ML) detector for ZF-PSM can be given by

$$\hat{\mathbf{x}} = \arg\min_{\mathbf{x}} \|\mathbf{y} - \beta_S\mathbf{x}\|^2 \tag{4}$$

Then, the average BER (ABER) for PSM systems can be obtained using the union bounding technique [23]. An upper bound on the ABER can be formulated as

$$\text{ABER} \leq \frac{1}{2^L}\sum_{i=1}^{2^L}\sum_{j=1}^{2^L}\frac{N\left(\mathbf{x}_i \to \mathbf{x}_j\right)}{L}E_{\mathbf{H}_S}\left\{\text{PEP}_S(\mathbf{x}_i \to \mathbf{x}_j)\right\} \tag{5}$$

where L is the total number of bits delivered in each transmission, $N(\mathbf{x}_i \to \mathbf{x}_j)$ is the number of bits in error between $\mathbf{x}_i$ and $\mathbf{x}_j$, and $\text{PEP}_S(\mathbf{x}_i \to \mathbf{x}_j)$ denotes the pairwise error probability (PEP) for a given $\mathbf{H}_S$ when $\mathbf{x}_i$ is transmitted but $\mathbf{x}_j$ is detected. From [9], the PEP for a given $\mathbf{H}_S$, i.e., β_S can be expressed as

$$\begin{aligned}\text{PEP}_S(\mathbf{x}_i \to \mathbf{x}_j) &= \Pr\left\{\|\mathbf{y}-\beta_S\mathbf{x}_i\|^2 > \left\|\mathbf{y}-\beta_S\mathbf{x}_j\right\|^2\right\}\\ &= Q\left(\sqrt{rSNR\left(S\right)}\,\left\|\mathbf{z}_{ij}\right\|^2\right)\end{aligned} \tag{6}$$

where

$$\mathbf{z}_{ij} = \mathbf{x}_i - \mathbf{x}_j \tag{7}$$

$$rSNR\left(S\right) = \frac{\beta_S^2}{2\sigma_n^2} \tag{8}$$

Here $rSNR\left(S\right)$ represents the received SNR for a given $\mathbf{H}_S$.

III. DIVERSITY ANALYSIS FOR ZF-PSM SYSTEM WITH TAS SELECTION

It is well-known in [24] and [25] that when there are N_T transmit antennas and N_R receive antennas, the diversity order of the ZF-PSM MIMO systems with no TAS selection is $N_T - N_R + 1$. To derive the transmit diversity order of the ZF-PSM system when using optimal TAS selection, the similar analysis approach carried out in [15] and [26] is employed after obtaining a tight bound of (6). Let S and S' be two TASs in the ZF-PSM systems, where $S \subset S' \subseteq \{1, 2, \cdots, N_T\}$. Using Lemmas presented in [20], β_S^2 can be represented as

$$\beta_S^2 = \frac{N_R}{Tr\left[\left(\mathbf{H}_{S'}\mathbf{H}_{S'}^H\right)^{-1}\right] + Tr\left(\mathbf{\Psi}_{\bar{S}}\right)} \tag{9}$$

where

$$\bar{S} = S' - S \tag{10}$$

$$\mathbf{\Psi}_{\bar{S}} = \mathbf{\Xi}_{S'}\mathbf{H}_{\bar{S}}\left(\mathbf{I}-\mathbf{H}_{\bar{S}}^H\mathbf{\Xi}_{S'}\mathbf{H}_{\bar{S}}\right)^{-1}\mathbf{H}_{\bar{S}}^H\mathbf{\Xi}_{S'} \tag{11}$$

$$\mathbf{\Xi}_{S'} = \left(\mathbf{H}_{S'}\mathbf{H}_{S'}^H\right)^{-1} \tag{12}$$

and $Tr\left(\mathbf{\Psi}_{\bar{S}}\right) > 0$. Then, we have

$$\beta_S^2 \leq \frac{N_R}{Tr\left[\left(\mathbf{H}_{S'}\mathbf{H}_{S'}^H\right)^{-1}\right]} = \beta_{S'}^2 \tag{13}$$

Further, it is shown that

$$\beta_S^2 = L_S\beta_{S'}^2 \tag{14}$$

where L_S is the ratio of the received SNR between two TASs of S and S' defined as

$$L_S \triangleq \frac{rSNR\left(S\right)}{rSNR\left(S'\right)} = \frac{\beta_S^2}{\beta_{S'}^2} = \frac{Tr\left[\left(\mathbf{H}_{S'}\mathbf{H}_{S'}^H\right)^{-1}\right]}{Tr\left[\left(\mathbf{H}_{S'}\mathbf{H}_{S'}^H\right)^{-1}\right] + Tr\left(\mathbf{\Psi}_{\bar{S}}\right)} \tag{15}$$

and under an assumption of fixed $Tr\left[\left(\mathbf{H}_{S'}\mathbf{H}_{S'}^H\right)^{-1}\right]$, it is less than 1 and a decreasing function as $Tr\left(\mathbf{\Psi}_{\bar{S}}\right)$ increases. It implies that increasing $Tr\left(\mathbf{\Psi}_{\bar{S}}\right)$ corresponds to decreasing $rSNR\left(S\right)$. That is, the received SNR of S is monotonically decreasing as the number $N_S(\leq N_T)$ of activated transmit antennas in ZF-PSM MIMO systems decreases. Hence, the expression of (15) denoted by L_S can be measured as *rSNR loss*, which is arising from a decrease in the number of active transmit antennas. In practical use, the values of L_S need to be numerically estimated and thus can be obtained on average through numerical simulations using TAS selection algorithms described in Section IV and are plotted in Fig. 6 of Section V, where its reciprocal is employed. Note that L_S can be regarded as a constant value for a specific simulation setup, in which case, it does not affect the diversity order, but the array gain. It is noticed that it is relatively small for large N_T and a quite small difference between N_S and N_T.

Then, the PEP of (6) can be rewritten as

$$\text{PEP}_S(\mathbf{x}_i \to \mathbf{x}_j) = Q\left(\sqrt{\frac{L_S\beta_{S'}^2}{2\sigma_n^2}}\,\left\|\mathbf{z}_{ij}\right\|^2\right) \tag{16}$$

By letting $S' = \{1, 2, \cdots, N_T\}$ and $|S| = N_T - 1$ for now, where S is a TAS selected optimally, the PEP of (16) satisfies

$$\text{PEP}_{S'}(\mathbf{x}_i \to \mathbf{x}_j) \leq \text{PEP}_S(\mathbf{x}_i \to \mathbf{x}_j) \tag{17}$$

where

$$\text{PEP}_{S'}(\mathbf{x}_i \to \mathbf{x}_j) = Q\left(\sqrt{\frac{\beta_{S'}^2}{2\sigma_n^2}}\,\left\|\mathbf{z}_{ij}\right\|^2\right) \tag{18}$$

It is pointed out that the value of L_S is small enough under the scenario with large N_T and $N_S = N_T - 1$. For example, the rSNR loss for $N_T = 16$ and $N_S = 15$ in Fig. 6 is obtained as about 0.0985 dB. It tells us that the difference between $\text{PEP}_{S'}(\mathbf{x}_i \to \mathbf{x}_j)$ and $\text{PEP}_S(\mathbf{x}_i \to \mathbf{x}_j)$ is quite small. Thus $\text{PEP}_{S'}(\mathbf{x}_i \to \mathbf{x}_j)$ could be used as a tight lower bound of $\text{PEP}_S(\mathbf{x}_i \to \mathbf{x}_j)$. Then $\text{PEP}_{S'}(\mathbf{x}_i \to \mathbf{x}_j)$ can be employed to obtain the diversity order of the ZF-PSM system with optimal TAS selection of $N_S = N_T - 1$. In Section IV, a decremental TAS selection algorithm successively eliminates $(N_T - N_S)$ transmit antennas one by one from the whole set of N_T transmit antennas during $(N_T - N_S)$ iterations. The rSNR loss produced by removing only one antenna at each iteration may be small if N_S is not relatively small, especially for the ZF-PSM system with large N_T. Furthermore, the diversity order is defined as the slope of BER in log-scale in the high SNR regime. At high SNR, the value of $rSNR\left(S\right)$ seems to approach that of $rSNR\left(S'\right)$. Hence, $\text{PEP}_{S'}(\mathbf{x}_i \to \mathbf{x}_j)$ can be adopted to derive the achievable diversity order of the ZF-PSM MIMO system with large antenna dimension. This work also uses the lower bound of (18) even for the MIMO system with small dimension, although it is presented for the large MIMO system.

By employing the Chernoff bound for Q function, $Q(x) \leq 0.5\exp(-x^2/2)$, the upper bound of (18) is given as

$$\mathrm{PEP}_{S'}(\mathbf{x}_i \rightarrow \mathbf{x}_j) \leq \frac{1}{2}\exp\left(-\frac{1}{4\sigma_n^2}\beta_{S'}^2 \left\| \mathbf{z}_{ij} \right\|^2\right) \tag{19}$$

Then, it is well-known that $\beta_{S'}^2$ has a Gamma distribution [9] and the diversity order is thus given by $N_T - N_R + 1$ [24], [25]. Therefore, the ZF-PSM MIMO system even using optimal TAS selection can achieve a diversity order of $G = N_T - N_R + 1$. It is equivalent to that of the ZF-PSM system using N_T transmit antennas and N_R receive antennas without TAS selection. However, it is observed from (8) and (9) that the loss of array gain in the ZF-PSM MIMO system using TAS selection occurs due to the additional term of $2\sigma_n^2 Tr\left(\boldsymbol{\Psi}_{\bar{S}}\right)$ in the expression of $rSNR\,(S)$.

IV. TAS SELECTION ALGORITHMS FOR ZF-PSM SYSTEMS

In ZF-based PSM MIMO systems, the received SNR is used as the design criterion for TAS selection. By adopting a reciprocal of (15), the received SNR expression of $\bar{S}\,(= S' - S)$ can be redefined in decibel as

$$\begin{aligned} rSNR_{dB}\left(\bar{S}\right) &= 10\log_{10}\left(rSNR\left(\bar{S}\right)\right) \\ &= 10\log_{10}\left(\frac{rSNR\left(S'\right)}{rSNR\left(S\right)}\right)\left(= 10\log_{10}\left(\frac{1}{L_S}\right)\right) \\ &= 10\log_{10}\left(1 + \frac{Tr\left(\boldsymbol{\Psi}_{\bar{S}}\right)}{Tr\left[\left(\mathbf{H}_{S'}\mathbf{H}_{S'}^H\right)^{-1}\right]}\right) \end{aligned} \tag{20}$$

As mentioned in Section III, if $Tr\left[\left(\mathbf{H}_{S'}\mathbf{H}_{S'}^H\right)^{-1}\right]$ is fixed, $rSNR_{dB}\left(\bar{S}\right)$ is positive and an increasing function with $Tr\left(\boldsymbol{\Psi}_{\bar{S}}\right)$. Since decreasing $Tr\left(\boldsymbol{\Psi}_{\bar{S}}\right)$ increases $rSNR\,(S)$, the received SNR of S is monotonically increasing with the number of active transmit antennas in ZF-PSM MIMO systems.

In the final analysis, let S_{opt1} and S_{opt2} denote two TASs of $\{1, 2, \cdots, N_T\}$ such that they have the maximum received SNR for $N_S = \left|S_{opt1}\right|$ and $N_S = \left|S_{opt2}\right|$, respectively. Then we have

$$\frac{rSNR\left(S_{opt1}\right)}{rSNR\left(S_{opt2}\right)} > 1 \quad \text{if } \left|S_{opt1}\right| > \left|S_{opt2}\right| \tag{21}$$

It implies that if the number of transmit antennas activated by TAS selection decreases, the corresponding maximum rSNR value is reduced at the same time. Thus, $rSNR_{dB}\left(\bar{S}\right)$ can be regarded as *rSNR loss in dB*, which is increasing from a reduction in the number of active transmit antennas and can be confirmed in Fig. 6 of Section V.

TABLE 1. Exhaustive search-based optimal TAS selection algorithm.

Procedure
Input: $\mathbf{H}_{S'}$
1: compute $\boldsymbol{\Xi}_{S'} = \left(\mathbf{H}_{S'}\mathbf{H}_{S'}^H\right)^{-1}$
2: for $k = 1 : C\left(N_T, N_S\right)$
3: $\bar{S}_k = S' - S_k$
4: $\boldsymbol{\Psi}_{\bar{S}_k} = \boldsymbol{\Xi}_{S'}\mathbf{H}_{\bar{S}_k}\left(\mathbf{I} - \mathbf{H}_{\bar{S}_k}^H\boldsymbol{\Xi}_{S'}\mathbf{H}_{\bar{S}_k}\right)^{-1}\mathbf{H}_{\bar{S}_k}^H\boldsymbol{\Xi}_{S'}$
5: $\beta_k = Tr\left(\boldsymbol{\Psi}_{\bar{S}_k}\right)$
6: end
7: $v = \arg\min_{k=1,2,\cdots,C(N_T,N_S)} \beta_k$
8: $\mathbf{H}_S = \mathbf{H}_{S_v}$
Output: $\mathbf{H}_S$

A. EXHAUSTIVE SEARCH-BASED OPTIMAL TAS SELECTION ALGORITHM

Minimizing the ABER of the ZF-PSM systems is equivalent to maximizing the term $rSNR\,(S)$. Furthermore, the optimal TAS that maximizes the $rSNR\,(S)$ corresponds to the TAS that minimizes the rSNR loss, $rSNR\left(\bar{S}\right)$. Hence, the TAS problem for the ZF-PSM systems can be described as

$$\begin{aligned} S_{opt} &= \underset{S\in\{S_k, k=1,2,\cdots,C(N_T,N_S)\}}{\arg\max} rSNR\,(S) \\ &= \underset{S\in\{S_k, k=1,2,\cdots,C(N_T,N_S)\}}{\arg\min} rSNR\left(\bar{S}\right) \end{aligned} \tag{22}$$

where S_k is the k-th enumeration of the set of all available $C\left(N_T, N_S\right)$ TASs. Here $C\left(N_T, N_S\right)$ is the total number of combinations of selecting N_S antennas among N_T transmit antennas. Based on (20), the TAS selection of (22) if $Tr\left[\left(\mathbf{H}_{S'}\mathbf{H}_{S'}^H\right)^{-1}\right]$ and N_R/σ_n^2 are fixed can be expressed as

$$S_{opt} = \underset{S\in\{S_k, k=1,2,\cdots,C(N_T,N_S)\}}{\arg\min} Tr\left(\boldsymbol{\Psi}_{\bar{S}}\right) \tag{23}$$

The exhaustive search-based optimal TAS selection algorithm of (23) is summarized in Table 1, where $S' = \{1, 2, \cdots, N_T\}$ and an input is given as $\mathbf{H}_{S'} = \mathbf{H} \in C^{N_R \times N_T}$.

It is pointed out that the computational complexity of (23) to find an optimal TAS is very high due to an exhaustive search when the number of transmit antenna combinations is large. To evaluate its computational complexity, we take account of the number of real multiplications (RMs) and the number of real summations (RSs) [25]. Here 4 RMs and 2 RSs are required for a complex multiplication whereas 2 RSs are used for a complex summation. From Table 1, the computational complexities of the exhaustive search-based TAS selection algorithm in terms of RMs and RSs, respectively, can be evaluated line by line as follows

Line 1:

- RM in $\mathbf{H}_{S'}\mathbf{H}_{S'}^H = 2N_TN_R^2 + 2N_TN_R$,

- RS in $\mathbf{H}_{S'}\mathbf{H}_{S'}^H = N_T N_R^2 + N_T N_R - N_R^2 - N_R$,
- RM in $(\cdot)^{-1} = 2N_R^3 + 6N_R^2$,
- RS in $(\cdot)^{-1} = N_R^3 - N_R^2$

Line 4:

- RM in $\boldsymbol{\Delta} = \boldsymbol{\Xi}_{S'}\mathbf{H}_{\bar{S}_k} = 4N_R^2(N_T - N_S)$,
- RS in $\boldsymbol{\Delta} = \boldsymbol{\Xi}_{S'}\mathbf{H}_{\bar{S}_k} = 2(N_R^2 - N_R)(N_T - N_S)$,
- RM in $\mathbf{H}_{\bar{S}_k}^H\boldsymbol{\Delta} = 2N_R(N_T - N_S)^2 + 2N_R(N_T - N_S)$,
- RS in $\mathbf{H}_{\bar{S}_k}^H\boldsymbol{\Delta} = (N_R - 1)(N_T - N_S)^2 + (N_R - 1)(N_T - N_S)$,
- RS in $\mathbf{I} - \mathbf{H}_{\bar{S}_k}^H\boldsymbol{\Delta} = N_T - N_S$,
- RM in $(\cdot)^{-1} = 2(N_T - N_S)^3 + 6(N_T - N_S)^2$,
- RS in $(\cdot)^{-1} = (N_T - N_S)^3 - (N_T - N_S)^2$,
- RM in $\boldsymbol{\Delta}\left(\mathbf{I} - \mathbf{H}_{\bar{S}_k}^H\boldsymbol{\Delta}\right)^{-1}\boldsymbol{\Delta}^H$
$= 4N_R(N_T - N_S)^2 + 2(N_R^2 + N_R)(N_T - N_S)$,
- RS in $\boldsymbol{\Delta}\left(\mathbf{I} - \mathbf{H}_{\bar{S}_k}^H\boldsymbol{\Delta}\right)^{-1}\boldsymbol{\Delta}^H$
$= 2N_R(N_T - N_S)^2 + (N_R^2 - N_R)(N_T - N_S) - N_R^2 - N_R$

Line 5:

- RS in $Tr(\cdot) = 2N_R$.

Thus the total complexities of the optimal TAS selection algorithm in terms of RMs and RSs, respectively, are given as

$$\begin{aligned} N_{exhaustive}^{RM} &= 2N_T N_R^2 + 2N_T N_R + 2N_R^3 + 6N_R^2 \\ &\quad + C\left(N_T, N_S\right) \times \Big(2\left(N_T - N_S\right)^3 + \left(6N_R + 6\right)\left(N_T - N_S\right)^2 \\ &\quad + \left(6N_R^2 + 4N_R\right)\left(N_T - N_S\right)\Big) \end{aligned} \tag{24}$$

$$\begin{aligned} N_{exhaustive}^{RS} &= N_T N_R^2 + N_T N_R + N_R^3 - 2N_R^2 - N_R \\ &\quad + C\left(N_T, N_S\right) \times \Big(\left(N_T - N_S\right)^3 + \left(3N_R - 2\right)\left(N_T - N_S\right)^2 \\ &\quad + \left(3N_R^2 - N_R\right)\left(N_T - N_S\right) + N_R - N_R^2\Big) \end{aligned} \tag{25}$$

B. DECREMENTAL TAS SELECTION ALGORITHM

To reduce the complexity of the optimal TAS algorithm in Table 1, a decremental antenna selection strategy is employed exploiting (23) together with (11). It starts with the whole set of N_T transmit antennas using an $N_R \times N_T$ full channel matrix $\mathbf{H}_{S'}$ $(= \mathbf{H})$ and successively removes $(N_T - N_S)$ transmit antennas during $(N_T - N_S)$ iterations. Because only one transmit antenna is eliminated at each iteration, the removed transmit antenna can be determined from

$$\hat{q} = \arg\min_{q} \frac{\left\| \mathbf{H}_{S_c}^H(:, q)\left(\mathbf{H}_{S_c}\mathbf{H}_{S_c}^H\right)^{-1} \right\|^2}{1 - \mathbf{H}_{S_c}^H(:, q)\left(\mathbf{H}_{S_c}\mathbf{H}_{S_c}^H\right)^{-1}\mathbf{H}_{S_c}(:, q)} \tag{26}$$

where S_c is the TAS employed at the current iteration and $\mathbf{H}_{S_c}(:, q)$ is the q-th column vector of the channel matrix $\mathbf{H}_{S_c}$ associated with the current iteration. Then the decremental TAS selection algorithm of (26) can be described as in Table 2.

TABLE 2. Decremental TAS selection algorithm.

Procedure
Inputs: $\mathbf{H}_{S'}, N_T, N_S$
1: $\mathbf{H}_t = \mathbf{H}_{S'}$
2: compute $\boldsymbol{\Xi}_t = \left(\mathbf{H}_t\mathbf{H}_t^H\right)^{-1}$
3: compute $\boldsymbol{\Pi}_t = \boldsymbol{\Xi}_t\boldsymbol{\Xi}_t^H$
4: for $p = 1, 2, \cdots, (N_T - N_S)$
5: for $q = 1, 2, \cdots, (N_T - p + 1)$
6: $\alpha_q = \dfrac{\mathbf{H}_t^H(:, q)\boldsymbol{\Pi}_t\mathbf{H}_t(:, q)}{1 - \mathbf{H}_t^H(:, q)\boldsymbol{\Xi}_t\mathbf{H}_t(:, q)}$
7: end
8: $\hat{q} = \arg\min_{q} \alpha_q$
9: $\boldsymbol{\Xi}_t = \boldsymbol{\Xi}_t + \dfrac{\boldsymbol{\Xi}_t\mathbf{H}_t(:, \hat{q})\mathbf{H}_t^H(:, \hat{q})\boldsymbol{\Xi}_t}{1 - \mathbf{H}_t^H(:, \hat{q})\boldsymbol{\Xi}_t\mathbf{H}_t(:, \hat{q})}$
10: $\mathbf{H}_t = \mathbf{H}_t(:, [1 : (\hat{q} - 1)\ \ (\hat{q} + 1) : \text{end}])$
11: end
12: $\mathbf{H}_S = \mathbf{H}_t$
Output: $\mathbf{H}_S$

From Table 2, the computational complexities of the decremental TAS selection algorithm in terms of RMs and RSs, respectively, can be analyzed line by line as

Line 2:

- RM in $\mathbf{H}_t\mathbf{H}_t^H = 2N_T N_R^2 + 2N_T N_R$,
- RS in $\mathbf{H}_t\mathbf{H}_t^H = N_T N_R^2 + N_T N_R - N_R^2 - N_R$,
- RM in $(\cdot)^{-1} = 2N_R^3 + 6N_R^2$,
- RS in $(\cdot)^{-1} = N_R^3 - N_R^2$

Line 3:

- RM in $\boldsymbol{\Xi}_t\boldsymbol{\Xi}_t^H = 2N_R^3 + 2N_R^2$,
- RS in $\boldsymbol{\Xi}_t\boldsymbol{\Xi}_t^H = N_R^3 - N_R$

Line 6:

- RM in $\mathbf{H}_t^H(:, q)\,\boldsymbol{\Pi}_t\,\mathbf{H}_t(:, q) = 4N_R^2 + 4N_R$,
- RS in $\mathbf{H}_t^H(:, q)\,\boldsymbol{\Pi}_t\,\mathbf{H}_t(:, q) = 2N_R^2 - 2$,
- RM in $\mathbf{H}_t^H(:, q)\,\boldsymbol{\Xi}_t\,\mathbf{H}_t(:, q) = 4N_R^2 + 4N_R$,
- RS in $\mathbf{H}_t^H(:, q)\,\boldsymbol{\Xi}_t\,\mathbf{H}_t(:, q) = 2N_R^2 - 2$

Line 9:

- RS in $\boldsymbol{\Xi}_t = \boldsymbol{\Xi}_t + (\cdot) = 2N_R^2$. Here, $\boldsymbol{\Xi}_t\mathbf{H}_t(:, \hat{q})$ and $\mathbf{H}_t^H(:, \hat{q})\,\boldsymbol{\Xi}_t\,\mathbf{H}_t(:, \hat{q})$ in $(\cdot)$ have been already computed in line 6.

Thus the total complexities of the decremental TAS selection algorithm in terms of RMs and RSs, respectively, are given as

$$\begin{aligned} N_{decremental}^{RM} &= \left(2N_T N_R^2 + 2N_T N_R + 4N_R^3 + 8N_R^2\right) \\ &\quad + \sum_{p=1}^{N_T - N_S} \left(N_T - p + 1\right)\left(8N_R^2 + 8N_R\right) \end{aligned} \tag{27}$$

TABLE 3. Computational complexity of RM and RS in different simulation scenarios.

SCENARIOS (N_T, N_S, N_R)	TAS ALGORITHM	RM	RS
(4,3,2)	OPTIMAL	296	74
	DECREMENTAL	304	84
(4,2,2)	OPTIMAL	1000	274
	DECREMENTAL	448	128
(6,4,2)	OPTIMAL	2392	664
	DECREMENTAL	664	188
(6,2,2)	OPTIMAL	8272	2524
	DECREMENTAL	1000	288
(6,5,4)	OPTIMAL	1328	406
	DECREMENTAL	1584	600
(6,4,4)	OPTIMAL	5864	2008
	DECREMENTAL	2384	932
(8,6,4)	OPTIMAL	10624	3660
	DECREMENTAL	3104	1212
(8,4,4)	OPTIMAL	74464	27348
	DECREMENTAL	4864	1936
(16,8,4)	OPTIMAL	49421664	19202388
	DECREMENTAL	17024	6664
(16,4,4)	OPTIMAL	16599264	6705228
	DECREMENTAL	21184	8352

$$N^{RS}_{decremental} = \left(N_T N_R^2 + N_T N_R + 2N_R^3 - 2N_R^2 - 2N_R\right) + \sum_{p=1}^{N_T - N_S} \left((N_T - p + 1)\left(4N_R^2 - 4\right) + 2N_R^2 \right) \tag{28}$$

Table 3 shows that the decremental TAS selection algorithm can effectively reduce the complexity compared to exhaustive search-based optimal TAS selection algorithm under various simulation scenarios, which are used in Section V. Especially, for the large dimension of multiple antennas, the complexity of the decremental TAS selection algorithm is tremendously lower than the exhaustive search-based optimal TAS selection algorithm. Nevertheless, note that the complexity of the proposed decremental algorithm is slightly larger than the optimal one for (4, 3, 2) and (6, 5, 4) scenarios, which has a relatively low dimension of multiple antennas together with $N_T - N_S = 1$.

V. SIMULATION RESULTS

This section shows through Monte Carlo simulations how the BER performance of the ZF-PSM systems varies due to TAS selection over Raleigh flat-fading channels. For the performance comparison, the ZF-based PSM system with optimal TAS selection (named opt-TAS) is compared with the ZF-PSM system with decremental TAS selection (named dec-TAS) and ZF-PSM system with no TAS selection (named no TAS). The SNR is defined by the symbol energy to the noise power spectral density ratio, i.e., $\eta = 1/\sigma_n^2$. The QPSK modulation is assumed. In the plots, (N_T, N_S, N_R) represents

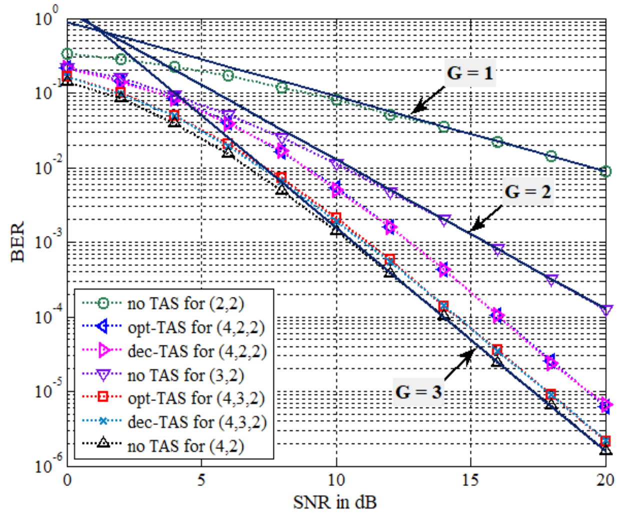

FIGURE 1. BER of optimal and decremental TAS selection algorithms for ZF-PSM system with $N_T = 4$ and $N_R = 2$.

using N_T transmit antennas, N_S selected transmit antennas, and N_R receive antennas as system parameters. On the other hand, (N_T, N_R) symbolizes no TAS selection. Furthermore, the BER reference curves are added into the same plots as a form of c/SNR^G with solid lines, where c is an appropriately selected positive constant and G denotes a diversity order, which determines a slope of BER curve.

Fig. 1 gives the BER performance of the ZF-PSM systems for $N_T = 4$ and $N_R = 2$ with optimal and decremental TAS selection. It is obvious that the ZF-PSM system with $N_T = 4$ and $N_R = 2$ outperforms the case with $N_T = 2$ and $N_R = 2$. The former can achieve the diversity order of 3 while the latter has no diversity. It is pointed out that the simulation results of no TAS selection for $(N_T, N_R) = (2, 2)$ and $(N_T, N_R) = (3, 2)$ are exactly matched with those of random TAS selection for $(N_T, N_S, N_R) = (4, 2, 2)$ and $(N_T, N_S, N_R) = (4, 3, 2)$, respectively. The random TAS selection scheme has no selection diversity, but if $N_S > N_R$, the transmit diversity is always available and then the diversity gain is given by $G = N_S - N_R + 1$, which corresponds to that of no TAS selection when $N_T > N_R$. Thus the diversity gain of random TAS selection is smaller than that of optimal and decremental TAS selection if $N_T > N_S$. Meanwhile, Fig. 2 shows the BER results for the case of $N_T = 6$ and $N_R = 2$. The diversity order of the ZF-PSM system with $N_T = 6$ and $N_R = 2$ is found to be 5 for no TAS selection. By comparing the BER results of $(N_T, N_R) = (4, 2)$ with those of $(N_T, N_R) = (6, 2)$, the latter outperforms the former due to the increased diversity gain. It is also seen that as the number of active transmit antennas decreases in opt-TAS or dec-TAS, the BER performance gets worse while still keeping the diversity order of $N_T - N_R + 1$. That is, the BER curves are shifted from left to right, which happen by increasing $2\sigma_n^2 Tr\left(\boldsymbol{\Psi}_{\bar{S}}\right)$ in denominator of $rSNR(S)$ expression (9) together with (8). In Fig. 1, the performance losses are about 0.6 dB for $N_S = 3$ and about 2 dB for $N_S = 2$. In Fig. 2, the rSNR losses are approximated

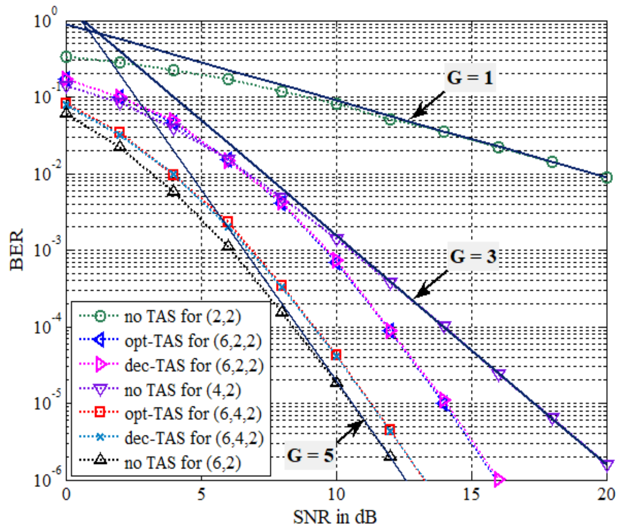

FIGURE 2. BER of optimal and decremental TAS selection algorithms for ZF-PSM system with $N_T = 6$ and $N_R = 2$.

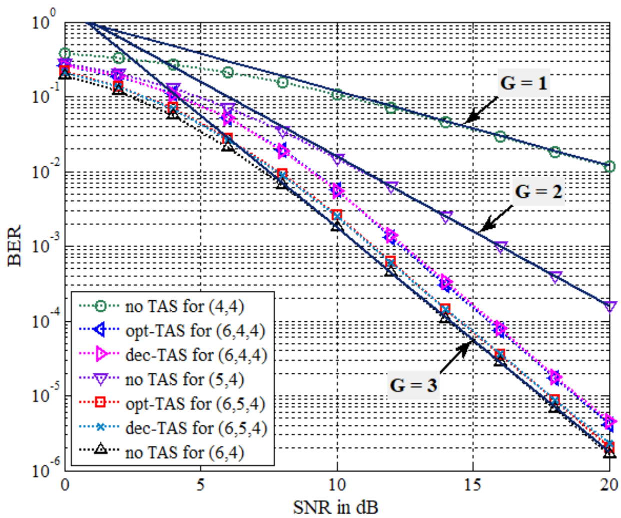

FIGURE 3. BER of optimal and decremental TAS selection algorithms for ZF-PSM system with $N_T = 6$ and $N_R = 4$.

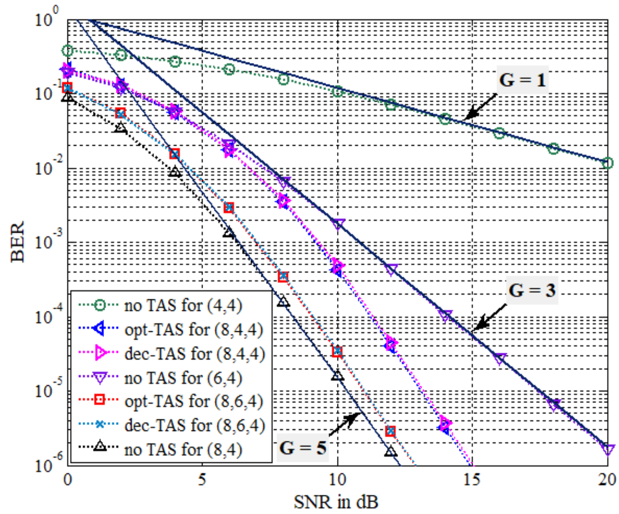

FIGURE 4. BER of optimal and decremental TAS selection algorithms for ZF-PSM system with $N_T = 8$ and $N_R = 4$.

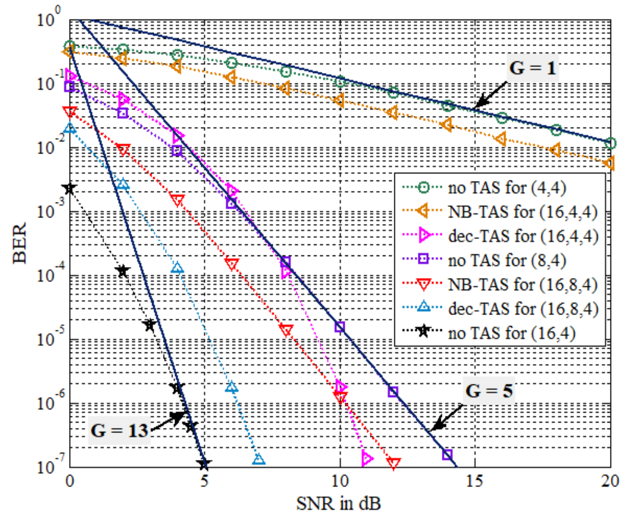

FIGURE 5. BER of decremental TAS selection algorithm for ZF-PSM system with $N_T = 16$ and $N_R = 4$.

by 0.77 dB for $N_S = 4$ and about 3.3 dB for $N_S = 2$. They are well-matched with analytical results in Fig. 6 plotted using (20), which represents the received SNR loss, $rSNR_{dB}(\bar{S})$, for the ZF-PSM system employing optimal and decremental TAS selection. On the other hand, the decremental TAS selection performance with low-complexity is very close to that of the optimal exhaustive TAS selection algorithm. To plot the BER reference curves, the constants selected for $G = 1, 2, 3$, and 5, are $c = 0.9, 1.28, 1.57$, and 1.97, respectively.

In Figs. 3 and 4, the scenarios of $N_T = 6$ and $N_T = 8$, respectively, for the ZF-PSM system with $N_R = 4$ are considered. It is shown that the BER performance decreases with decreasing N_S and the decremental TAS selection can achieve almost a similar performance to optimal TAS selection. By comparing Fig. 3 with Fig. 4, even if there exist performance losses due to optimal or decremental TAS selection, the ZF-PSM system with $(N_T, N_S, N_R) = (8, 4, 4)$ is seen to offer better performance than the (6, 4, 4) system. It is because the one has the diversity order of 5 while the other has 3. It is also found that the received SNR losses are close to analytical results presented in Fig. 6. For the BER reference curves in Figs. 3 and 4, the constants, $c = 1.2, 1.58, 1.77$, and 1.5, are used for $G = 1, 2, 3$, and 5, respectively.

Fig. 5 considers the ZF-PSM system with $N_T = 16$ and $N_R = 4$, where the selected number of transmit antennas is 4 and 8. As shown in Table 3, the optimal TAS selection algorithm requires huge computational complexity for this case, thus we present the simulation results of only the decremental TAS selection algorithm with enormous reduction of complexity. It is found that the given simulated ZF-PSM system can achieve the diversity order of 13. For the BER reference curves, the constants, $c = 1.2, 1.5$, and 0.37, are selected for $G = 1, 5$, and 13, respectively. For comparison purpose, simulation results of a simple norm-based TAS (NB-TAS)

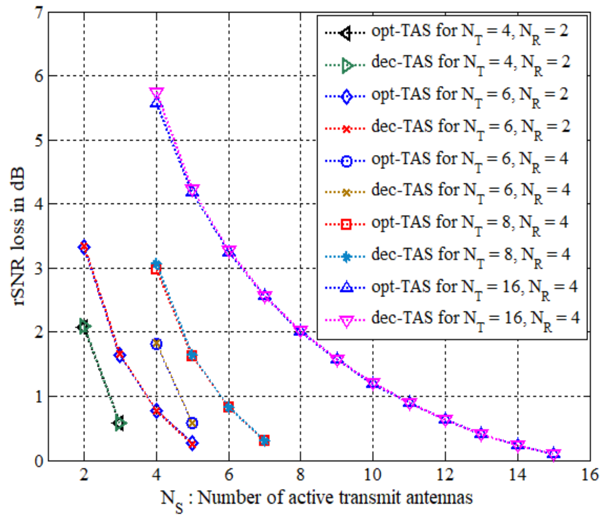

FIGURE 6. Received SNR loss for ZF-PSM system with TAS selection.

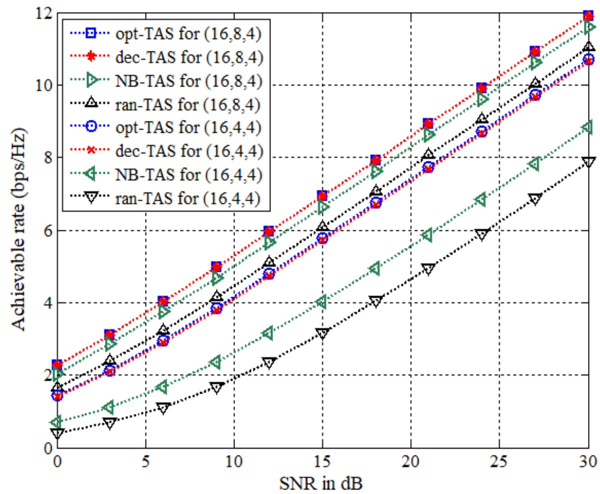

FIGURE 7. Achievable rate of TAS selection algorithms for ZF-PSM system with $N_T = 16$ and $N_R = 4$.

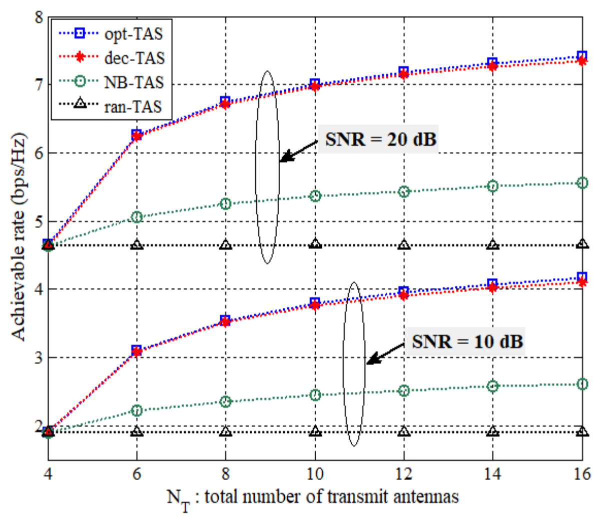

FIGURE 8. Achievable rate of TAS selection algorithms for ZF-PSM system with $N_S = 4$ and $N_R = 4$.

algorithm [22] are also presented, which selects N_S antennas out of N_T transmit antennas that correspond to the N_S columns, which have the largest Frobenius norm among N_T columns of the channel matrix $\mathbf{H}$. The dec-TAS outperforms the NB-TAS. The SNR degradation found in Fig. 5 is close to the analytical results in Fig. 6. By comparing both SNR losses in Figs. 5 and 6, it is anticipated that the decremental TAS selection algorithm approaches the BER performance of the optimal TAS selection one, which is not presented here due to huge computations, for the ZF-PSM system with $N_T = 16$ and $N_R = 4$. From these results, we can apply the analytical results to massive MIMO cases with optimal or decremental TAS selection. Thus the received SNR loss of massive MIMO systems, which happens from decreasing the number of active transmit antennas, can be easily obtained by numerical results of (20).

To examine the achievable rate behavior of the ZF-PSM system with TAS selection, the following achievable rate R_S is considered [28]–[30].

$$R_S = \log_2 \left(1 + rSNR\,(S) \right) \tag{29}$$

where $rSNR\,(S)$ is the received SNR based on the selected channel $\mathbf{H}_S$, which is given in (8). In Figs. 7 and 8, ran-TAS denotes random TAS selection for (N_T, N_S, N_R) and actually corresponds to no TAS selection for (N_T, N_R) where $N_T = N_S$ as mentioned before. Fig. 7 depicts the achievable rate as function of SNR values for the ZF-PSM system with $N_T = 16$ and $N_R = 4$. It is observed that the proposed decremental TAS selection scheme achieves the transmission rate corresponding to the optimal TAS selection algorithm for both $N_S = 8$ and $N_S = 4$, which is larger than those of NB-TAS and ran-TAS selection. Furthermore, it is obvious that the $(N_T, N_S, N_R) = (16, 8, 4)$ system gives better performance than the $(N_T, N_S, N_R) = (16, 4, 4)$. In Fig. 8, the achievable rate of the ZF-PSM system with $N_S = 4$ and $N_R = 4$ is shown as a function of N_T for two SNR values such as 10 dB and 20 dB. The decremental TAS selection algorithm is able to achieve the performance of optimal TAS selection with much lower complexity. The achievable rate of opt-TAS and dec-TAS increases with almost similar performance as the number of transmit antennas available increases. The NB-TAS performs worse than the opt-TAS and dec-TAS. On the other hand, the rate performance of ran-TAS selection is not affected by the total number of transmit antennas.

VI. CONCLUSION

In this paper, TAS selection is considered to reduce the use of RF units in the transmitter of PSM-MIMO systems. It is analyzed that decreasing the number of activated RF units lowers the received SNR of a selected TAS. The received SNR loss derived analytically agrees with simulation results. An optimal TAS selection criterion based on exhaustive search is presented to minimize the received SNR loss by TAS selection. To obtain a TAS selection algorithm with complexity reduction, a decremental selection scheme is proposed.

The complexity analysis shows that the computational complexity of the decremental TAS algorithm is tremendously lower than that of the optimal one, especially for large antenna systems. That is, the decremental TAS algorithm with low-complexity can achieve almost the same BER and achievable rate performance as optimal one. In addition, reducing the number of active transmit antennas by optimal and decremental TAS selection causes the received SNR loss, which shifts the BER curve from left to right, while still keeping the same transmit antenna diversity order of $G (= N_T - N_R + 1)$ as the under-determined ZF-based PSM MIMO system with N_T transmit antennas and N_R receive antennas without TAS selection.

REFERENCES

[1] R. Y. Mesleh, "Spatial modulation," *IEEE Trans. Veh. Technol.*, vol. 57, no. 4, pp. 2228–2241, Jul. 2008.
[2] M. Renzo, H. Haas, and P. Grant, "Spatial modulation for multiple-antenna wireless systems: A survey," *IEEE Commun. Mag.*, vol. 49, no. 12, pp. 182–191, Dec. 2011.
[3] J. Jeganathan, A. Ghrayeb, and L. Szczecinski, "Spatial modulation: Optimal detection and performance analysis," *IEEE Commun. Lett.*, vol. 12, no. 8, pp. 545–547, Aug. 2008.
[4] L.-L. Yang, "Transmitter preprocessing aided spatial modulation for multiple-input multiple-output systems," in *Proc. IEEE 73rd Veh. Technol. Conf. (VTC Spring)*, May 2011, pp. 1–5.
[5] R. Zhang, L.-L. Yang, and L. Hanzo, "Generalised pre-coding aided spatial modulation," *IEEE Trans. Wireless Commun.*, vol. 12, no. 11, pp. 5434–5443, Nov. 2013.
[6] P. Yang, Y. L. Guan, Y. Xiao, M. D. Renzo, S. Li, and L. Hanzo, "Transmit precoded spatial modulation: Maximizing the minimum Euclidean distance versus minimizing the bit error ratio," *IEEE Trans. Wireless Commun.*, vol. 15, no. 3, pp. 2054–2068, Mar. 2016.
[7] C. Liu, L.-L. Yang, and W. Wang, "Transmitter-precoding-aided spatial modulation achieving both transmit and receive diversity," *IEEE Trans. Veh. Technol.*, vol. 67, no. 2, pp. 1375–1388, Feb. 2018.
[8] Y. Cao, T. Ohtsuki, and X.-Q. Jiang, "Precoding aided generalized spatial modulation," *IEEE Access*, vol. 6, pp. 72449–72457, 2018.
[9] J. Luo, S. Wang, F. Wang, and W. Zhang, "Generalized precoding-aided spatial modulation via receive antenna transition," *IEEE Wireless Commun. Lett.*, vol. 8, no. 3, pp. 733–736, Jun. 2019.
[10] A. F. Molisch and M. Z. Win, "MIMO systems with antenna selection-an overview," *IEEE Microw. Mag.*, vol. 5, no. 1, pp. 46–56, Mar. 2004.
[11] S. Asaad, A. M. Rabiei, and R. R. Müller, "Massive MIMO with antenna selection: Fundamental limits and applications," *IEEE Trans. Wireless Commun.*, vol. 17, no. 12, pp. 8502–8516, Dec. 2018.
[12] B. Gäde, A. Beryhi, S. Asaad, and R. R. Müller, "A fair comparison between spatial modulation and antenna selection in massive MIMO systems," in *Proc. 23rd Int. ITG Workshop Smart Antennas*, Apr. 2019, pp. 1–6.
[13] R. Rajashekar, K. V. S. Hari, and L. Hanzo, "Antenna selection in spatial modulation systems," *IEEE Commun. Lett.*, vol. 17, no. 3, pp. 521–524, Mar. 2013.
[14] N. Pillay and H. Xu, "Comments on 'Antenna selection in spatial modulation systems,"' *IEEE Commun. Lett.*, vol. 17, no. 9, pp. 1681–1683, Sep. 2013.
[15] R. Rajashekar, K. V. S. Hari, and L. Hanzo, "Quantifying the transmit diversity order of Euclidean distance based antenna selection in spatial modulation," *IEEE Signal Process. Lett.*, vol. 22, no. 9, pp. 1434–1437, Sep. 2015.
[16] J. Zheng, "Fast receive antenna subset selection for pre-coding aided spatial modulation," *IEEE Wireless Commun. Lett.*, vol. 4, no. 3, pp. 317–320, Jun. 2015.
[17] P. Wen, X. He, Y. Xiao, P. Yang, R. Shi, and K. Deng, "Efficient receive antenna selection for pre-coding aided spatial modulation," *IEEE Commun. Lett.*, vol. 22, no. 2, pp. 416–419, Feb. 2018.
[18] D. A. Gore, R. U. Nabar, and A. Paulraj, "Selecting an optimal set of transmit antennas for a low rank matrix channel," in *Proc. IEEE Int. Conf. Acoust., Speech, Signal*, vol. 5, Jun. 2000, pp. 2785–2788.
[19] S.-H. Tsai, "Equal gain transmission with antenna selection in MIMO communications," *IEEE Trans. Wireless Commun.*, vol. 10, no. 5, pp. 1470–1479, May 2011.
[20] P.-H. Lin and S.-H. Tsai, "Performance analysis and algorithm designs for transmit antenna selection in linearly precoded multiuser MIMO systems," *IEEE Trans. Veh. Technol.*, vol. 61, no. 4, pp. 1698–1708, May 2012.
[21] S. Huang, H. Yin, H. Li, and V. C. M. Leung, "Decremental user selection for large-scale multi-user MIMO downlink with zero-forcing beamforming," *IEEE Wireless Commun. Lett.*, vol. 1, no. 5, pp. 480–483, Oct. 2012.
[22] S. Kim, "Performance of decremental antenna selection algorithms for spatial multiplexing MIMO systems with linear receiver over correlated fading channels," *IET Commun.*, vol. 11, no. 6, pp. 855–863, Apr. 2017.
[23] M. K. Simon and M.-S. Alouini, *Digital Communication over Fading Channels*, 1st ed. Hoboken, NJ, USA: Wiley, 2000.
[24] Y. Jiang, M. K. Varanasi, and J. Li, "Performance analysis of ZF and MMSE equalizers for MIMO systems: An in-depth study of the high SNR regime," *IEEE Trans. Inf. Theory*, vol. 57, no. 4, pp. 2008–2026, Apr. 2011.
[25] J. H. Winters, J. Salz, and R. D. Gitlin, "The impact of antenna diversity on the capacity of wireless communication systems," *IEEE Trans. Commun.*, vol. 42, nos. 2–4, pp. 1740–1751, Feb./Apr. 1994.
[26] S. Kim, "Diversity order of precoding-aided spatial modulation using receive antenna selection," *Electron. Lett.*, vol. 56, no. 5, pp. 260–262, Mar. 2020.
[27] R. Hunger, "Floating point operations in matrix-vector calculus (Version 1.3)," Technische Universität München, München, German, Tech. Rep., 2007. [Online]. Available: https://mediatum.ub.tum.de/doc/625604/625604.pdf
[28] Y. Huang, M. Wen, B. Zheng, X. Cheng, L. Yang, and F. Ji, "Secure precoding aided spatial modulation via transmit antenna selection," *IEEE Trans. Veh. Technol.*, vol. 68, no. 9, pp. 8893–8905, Sep. 2019.
[29] M. Maleki, K. Mohamed-Pour, and M. Soltanalian, "Large-system mutual information analysis of receive spatial modulation in correlated multi-cell massive MIMO networks," *IEEE Trans. Commun.*, vol. 67, no. 9, pp. 6071–6084, Sep. 2019.
[30] T. Brown, E. D. Carvalho, and P. Kyritsi, *Practical Guide to the MIMO Radio Channel With MATLAB Examples*, 1st ed. Chichester, U.K.: Wiley, 2012.

SANGCHOON KIM was born in Jeju, South Korea, in 1965. He received the B.S. degree in electrical and computer engineering from Yonsei University, Seoul, South Korea, in 1991, and the M.E. and Ph.D. degrees in electrical and computer engineering from the University of Florida, Gainesville, FL, USA, in 1995 and 1999, respectively. From 2000 to 2005, he was a Senior Research Engineer at LG Corporate Institute of Technology, Seoul, and a Chief Research Engineer with LG Electronics, Anyang, South Korea, working on a range of research projects in the field of wireless/mobile communications. In 2005, he joined Dong-A University, Busan, South Korea, where he is currently a Professor with the Department of Electronics Engineering. His research interests include a range of areas in wireless/mobile communications, signal processing, and antenna design.